The 2010 IEEE/RSJ International Conference on
Intelligent Robots and Systems
October 18-22, 2010, Taipei, Taiwan

An Articulated Rehabilitation Robot for Upper Limb Physiotherapy and Training

B.-C. Tsai, W.-W. Wang, L.-C. Hsu, L.-C. Fu and J.-S. Lai

Abstract—**The objective of this study is to design a robot system to assist the rehabilitation of patients so that they can afterwards do various daily activities. It is difficult to determine the desirable posture of a 9-DOFs exoskeleton manipulator in such a system and each joint control design as well. In this paper, we resolve the difficulties by mapping the kinematics of a human arm to that of the manipulator so that we can avoid going through the ill-postured configurations while searching for the desired solutions, and then reach the desired rehabilitation motion as precisely as possible. In addition, this study combines electromyography (EMG) and force sensor to detect the patient's motion on his/her volition, so that the rehab-robot can support the human's upper limb appropriately to fulfill the intended motion. For validation of our rehab-robot design, experiments are conducted and promising results are obtained.**

I. Introduction

For over a decade of development, rehabilitation robots (rehab-robots) for physiotherapy have been put to use so far. In fact, many rehab-robots in the literature [1-4] have been proposed for upper limb therapy and assistance. According to the mechanical structure of the rehab-robots, there are mainly three types which contact or interact with stroke patients. The first type is an endpoint-fixation system, such as MIT-Manus [1], that can fix the distal part of UE of patients to guide the desired movements. That is, stroke patients can execute a task by use of only forearm support. The second type is a cable suspension system, such as Freebal gravity compensation system [2]. It provides antigravity support for the UE during rehabilitation. The third type is an exoskeleton arm system, such as ARMin [3].

In this study, our rehab-robot is chosen to be of exoskeleton type. The use of redundancy for the generation of human-like robot arm (exoskeletons) has been already proposed in the literature and a variety of proposed cost functions has been suggested to explain the principles of the human arm movements. All these structures of human-like robots usually adopted some special component which is a circular guide or a ring to attain to human shoulder's internal/external rotation. However, design of the special component is involved. The study here aims to use the coordinate function and biologically inspired criterion to attain our goal in imitating human's motion.

This rehab-robot is designed for exoskeleton-type for upper extremities rehabilitation, and it include the redundancy design combined with selective inverse kinematics (IK) solutions, the impedance control [4-6], and the EMG-trigger modified from MIT-Manus [7]. Among them, the redundancy design refers to more joints than normal human's upper limb. This design can lead to ROM closer to that of a normal human and provide coordinate mechanical structure. Because the IK problem arises from the redundancy design, an attempt in this research is to first study the geometrical relationship between the robot arm and the human arm and then to seek an effective or the optimal IK solution for it.

An application of the developed rehab-robot to stroke rehabilitation is to perform circle drawing. It is a training program to execute the coordinated movements with the paretic arm. Miyoshi et el. (2010) pointed out that it is a complex movement that coordinates the muscular co-contraction and eccentric activity [8] in the medial/ lateral and forward/ backward directions. Besides, a significant relationship between activation of the motor cortex and copying of the visual presentation of some geometrical shape [9] has been reported.

II. Design of Rehab-Robot

A. Mechanical structure

The degree of freedom (DOF) of human's upper limb is typically defined as the total number of independent displacements or motion. Generally speaking, there are 3-DOF movements at the shoulder joint complex (flexion/ extension, abduction/ adduction, internal / external rotation), 2-DOF at the elbow joint (flexion/ extension, forearm pronation/ supination), and 2-DOF at the wrist joint (flexion/ extension, medial/ lateral deviation). Ideally, designing 7 D.O.F. upper limbs rehab-robot can reach all of the features, but in fact, it cannot achieve because it shall produce some dead zone of range of motion (ROM), shoulder especially. So we use the redundancy design to resolve this question.

The multiple degrees of freedom of the rehab-robot are designed to provide more alternative kinematic solutions

This work was supported in part by National Science Council, R.O.C., via contracts: NSC 94-2218-E-002-075, NSC 95-2218-E-002-039, and NSC 96-2218-E002-008, and in part by National Taiwan University Hospital via contracts: aNTUH.97A20.

B.-C. Tsai is with Department of Electrical Engineering, National Taiwan University, R.O.C. (e-mail: r97921006@ntu.edu.tw).

W.-W. Wang is with Department of Electrical Engineering, National Taiwan University, R.O.C. (e-mail: d94921007@ntu.edu.tw).

L.-C. Hsu is with Department of Electrical Engineering, National Taiwan University, R.O.C. (e-mail: r98921004@ntu.edu.tw).

L.-C. Fu is with the Department of Electrical Engineering, National Taiwan University, R.O.C. (e-mail: lichen@ntu.edu.tw).

J.-S. Lai is with the Department of Physical Medicine and Rehabilitation, National Taiwan University (NTU) and NTU Hospital, R.O.C. (e-mail: jslai@ntu.edu.tw).

while simultaneously rejecting unfavorable singularity points in the associated workspace. Following such conception, the exoskeleton-type robot arm is equipped with more joints than a human arm, resulting in a 9 DOF mechanical manipulator, including 6-DOF at the shoulder joint complex, 1-DOF at the elbow joint, and 2-DOF at the wrist joint, as shown in Fig. 1.

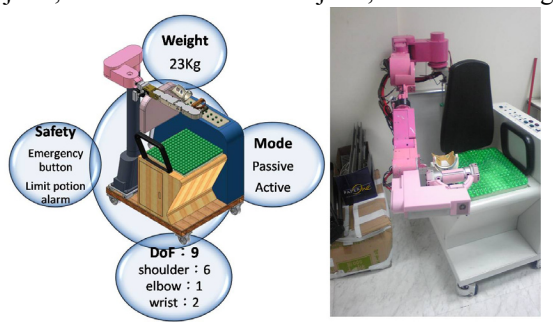

Fig. 1. The picture of the rehab-robot

In the following, Fig. 2 shows the movement freedom of a human's upper limb and its association with the mentioned 9 DOF rehab-robot. Apparently, the mechanical joints 1~6 of the rehab-robot are used to accommodate the motions due to the human's shoulder joint (namely, joints 2~4 for the horizontal plane movements, joint 5 for the sagittal plane movements, joints 1,2,3,4,6 for the internal/ external rotations), the mechanical joint 7 is used to accommodate the motions due to the human's elbow joint, and the remaining mechanical joints are used to accommodate the motions due to the human wrist joint (that is, joints 8~9 for the pronation/ supination movements). In order to make the robot adaptable to different patient subjects, its mechanism is designed such that the length of the upper arm can be made to vary from 26 cm to 34 cm whereas that of the forearm can be made to vary between 24 cm and 30 cm.

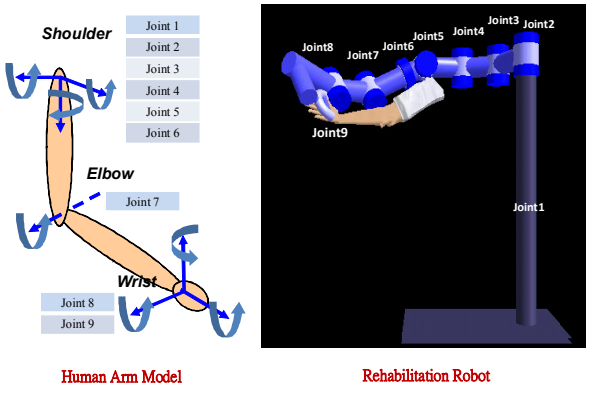

Fig. 2. The motion model of human upper limb (a) a human arm model (b) a rehabilitation robot

B. *System Architecture*

According to the general functions of a control system, it can be divided into three categories: (1) sensor system, (2) actuator device and (3) computer based processor. The sensor system typically includes potentiometer, motor encoder for each joint, and electromyography (EMG) and force sensors for human's upper limb. The electrode pairs are attached to the surface of the muscles to collect the patient subject's EMG signals.

Besides, the rehab-robot is equipped with 4 force sensors mounted on the connections between the robot and the human arm, as shown in Fig. 3. Each force sensor is realized by a pair of strain gage used to measure the interaction force between the human and robot. The force measured from the upper arm by two force sensors is due to shoulder flexion/extension and horizontal adduction/abduction. Whereas, the elbow flexion/extension with shoulder rotation yields interaction force measured form the forearm. On the other hand, the potentiometer at each joint of the rehab-robot outputs the absolute joint position information of that particular joint. But, for the sake of attaining more accurate position and/or speed control, additional motor encoder is attached to each joint motor to extract the information of the relative joint position of the associated joint with higher resolution. The actuator devices utilize DC motors of FAULHABER series, which have significant features of light weight and high torque.

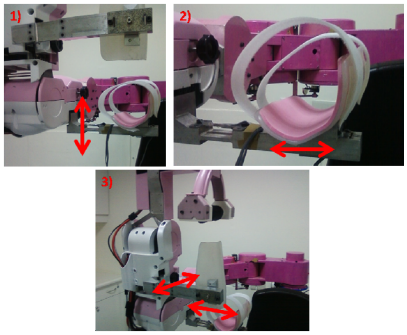

Fig. 3. There are four force sensors mounted on the robot arm. The sensor shown in photo 1) can sense the force of shoulder flexion/extension. Photo 2) shows the sensor which can sense the force of shoulder and horizontal adduction/abduction. The structure of forearm's sensor is similar to upper arm and can sense the forces of flexion/extension and shoulder rotation.

III. KINEMATICS OF REHAB-ROBOT

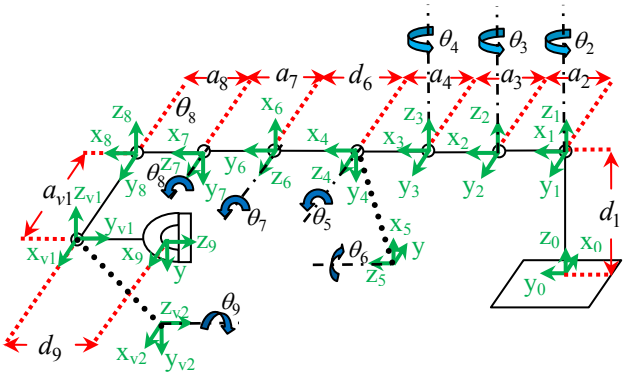

Fig. 4. The 9 DOF rehab-robot arm

In this section, we will try to explore all feasible motions of this 9 DOF exoskeleton-type rehab-robot arm through the

study of its inverse kinematic solutions. To meet this purpose, a simplified schematic diagram of the robot structure is drawn in Fig. 4, where totally 12 coordinate frames are assigned to the base and appropriate locations on the 11 joint axes using Denavit-Hartenberg (D-H) notation. In the sequel, we will call the origins of the coordinate frames as "joint pivots" for convenience. Note that the joints V_1 (Z_8) and joints V_2 (Z_{V1}) are stationary, and hence the associated rotating angles θ_{V1} and θ_{V2} are constant, leading to a U link connecting the arm at the origin of the coordinate frame {XYZ_7} and the handle for grasping at the origin of the coordinate frame {XYZ_9}. Later, the notations d_1 (with sliding joint) and $\theta_2 \sim \theta_9$ (with revolute joints) are treated as variables that correspond to various joint motions, and the associated D-H parameters are shown in Table I.

TABLE I

DH PARAMETERS OF REHABILITATION ROBOT

Joint	θ	d(cm)	a(cm)	α (rad.)	Home (rad.)
1	0	d_1	0	0	π/2
2	θ_2	0	a_2	0	0
3	θ_3	0	a_3	0	0
4	θ_4	0	a_4	-π/2	0
5	θ_5	0	0	-π/2	-π/2
6	θ_6	d_6	0	π/2	0
7	θ_7	0	a_7	0	π/2
8	θ_8	0	a_8	π/2	0
V1	θ_{V1}	0	a_{V1}	0	π/2
V2	θ_{V2}	0	0	-π/2	0
9	θ_9	d_9	0	0	0

Because our design of the rehab-robot belongs to the exoskeleton-type, it is legitimate to assume that in normal operation the human arm is basically posed in parallel with the rehab-robot arm, which naturally infers that the trajectories of some joint pivots of the robot should be kept in appropriate relationship with those of some corresponding joints of the human arm. Based on this parallel-motion principle, instead of solving the inverse kinematic solutions generally and finding the entire motion space of the robot, we simplify this problem by finding only those solutions such that both the rehab-robot and the human arm will conform to the above-mentioned principle. Technically speaking, we will first try to find the position trajectories of the essential joint pivots of the rehab-robot given the knowledge of those of various joints of the human arm. More specifically, we just find three positions of the robot's joint pivots which correspond to human's shoulder joint, elbow joint, and wrist joint. In turn, we can easily solve the pose of the rehab-robot by geometry based on these three found positions.

Suppose that we know the desired positions of the human's shoulder joint O_{hs}, elbow joint O_{he}, wrist joint O_{hw}, the length of upper arm l_{hse}, the length of forearm l_{hew}, and the parallel distance l_{hr} between rehab-robot and human arm. Denote the pivots of joint 1 to joint 9 of the robot arm as O_1 to O_9, and in particular rename the pivots of joint 4, joint 6 and joint 7 as robot's shoulder joint $O_{rs}(=O_4)$, elbow joint $O_{re}(=O_6)$, and wrist joint $O_{rw}(=O_7)$, respectively. Complying with the formerly mentioned principle, the latter three robot joints should corresponded to the joints O_{hs}, O_{he}, and O_{hw} of the human arm, respectively. Now, if we further denote the lengths of robot's upper arm and robot's forearm as $l_{rse}(=d_6)$ and $l_{rew}(=a_7)$, respectively, we can characterize the relationship between the human arm and the robot from what are shown in Fig. 5 below.

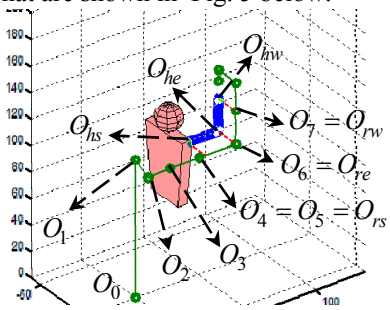

Fig. 5. The relationship between the robot and human.

In general, we can adjust the lengths of robot's upper arm and robot's forearm to match the lengths of human's counterparts. But we prefer to let the length of robot's upper arm be longer than that of human's in order to accommodate the petite patients while solving the inverse kinematic problem optimally. Now, we will start to derive the solution as follows.

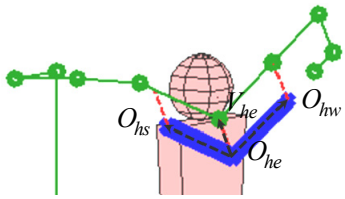

Fig. 6. Figure showing a relationship among human's shoulder, elbow and wrist joints, defining the vector of elbow V_{he}, a vector normal to the plane containing the three joint positions.

At first, we shall find the position of the robot's elbow joint O_{re} when the pose of the human arm is given. From Fig. 6, we define the vectors of human upper arm $V_{hes} = O_{hs} - O_{he}$ and forearm $V_{hew} = O_{hw} - O_{he}$, which later can be used to derive the vector of elbow V_{he} :

$$V_{he} = V_{hew} \times V_{hes} = [\bar{x}_{he} \quad \bar{y}_{he} \quad \bar{z}_{he}]^T \tag{1}$$

Following the parallel-motion principle introduced previously, the robot's elbow joint O_{re} should be situated along the direction of V_{he} from the human's elbow joint O_{he}, i.e.,

$$O_{re} = O_{he} + l_{hr} \cdot V_{he} / |V_{he}| \tag{2}$$

Then, it is straightforward to compute the position of the robot's shoulder joint once the position of the robot's elbow joint is found. This is because the vector of the robot's upper arm V_{res} is parallel to the vector of the human's upper arm V_{hes}, and we can then directly determine the robot's shoulder joint as :

$$O_{rs} = O_{re} + l_{res} \cdot V_{hes} / |V_{hes}| \tag{3}$$

Now, there are positions of the robot's shoulder and elbow, so we can find the suitable solution of I.K. from the geometry in Fig 7. The result is show in following formulas.

$$\theta_{hsew} = \cos^{-1}\left(\frac{V_{hes} \cdot V_{hew}}{|V_{hes}| \cdot |V_{hew}|}\right) \tag{4}$$

$$\theta_7 = \theta_{hsew} - \pi \tag{5}$$

$$V_{he0} = \begin{bmatrix} -(y_{he} - y_{hs}) \\ x_{he} - x_{hs} \\ 0 \end{bmatrix} \tag{6}$$

$$\theta_{hs3} = sign(\bar{z}_{he}) \cdot \cos^{-1}\left(\frac{V_{he0} \cdot V_{he}}{|V_{he0}| \cdot |V_{he}|}\right) \tag{7}$$

$$\theta_6 = -sign(\bar{z}_{he}) \cdot \cos^{-1}\left(\frac{V_{he0} \cdot V_{he}}{|V_{he0}| \cdot |V_{he}|}\right) \tag{8}$$

$$\theta_5 = atan2\left(\sqrt{(x_{rs} - x_{re})^2 + (y_{rs} - y_{re})^2}, z_{rs} - z_{re}\right) \tag{9}$$

$$\theta_{hs1} = \pi - atan2(x_{he} - x_{hs}, y_{he} - y_{hs}) \tag{10}$$

$$O_3 = \begin{bmatrix} x_3 \\ y_3 \\ z_3 \end{bmatrix} = \begin{bmatrix} x_{rs} + a_4 \cdot \cos\theta_{hs1} \\ y_{rs} - a_4 \cdot \sin\theta_{hs1} \\ z_{rs} \end{bmatrix} \tag{11}$$

$$\cos\theta_3 = \frac{x_3^2 + y_3^2 - a_2^2 - a_3^2}{2 \cdot a_2 \cdot a_3} \triangleq D \tag{12}$$

$$\theta_3 = atan2(D, \pm\sqrt{1 - D^2}) \tag{13}$$

$$\theta_2 = atan2(x_3, y_3) - atan2(a_2 + a_3\cos\theta_3, a_3\sin\theta_3) \tag{14}$$

$$\measuredangle y_2 O_2 O_3 = \pi - (\theta_2 + \theta_3) \tag{15}$$

$$\theta_4 = \measuredangle y_2 O_2 O_3 - \theta_{rs1} \tag{16}$$

$$d_1 = z_{rs} \tag{17}$$

Finally, because we limit the motion of human wrist (flexion/ extension, abduction/ adduction, and pronation/ supination of the forearm) to simple motions, the joints of the human wrist and the corresponding joints of the robot (θ_8 and θ_9) are simply coaxial, i.e., their solutions are straightforward.

To sum up, the foregoing solution of I.K. can be divided into two groups. The first of which concerns angles of $\theta_1 \sim \theta_6$ whereas the second one concerns angles of $\theta_7 \sim \theta_9$. In the first group, we try to find the pose of the robot after the posture of robot's elbow is calculated based on the pose of the human arm. The solution of the second group directly corresponds to angles of the human arm when $\theta_1 \sim \theta_6$ in the first group of solution are determined. Because we divide the overall solution of I.K. into two groups, the burden of calculation can be greatly reduced.

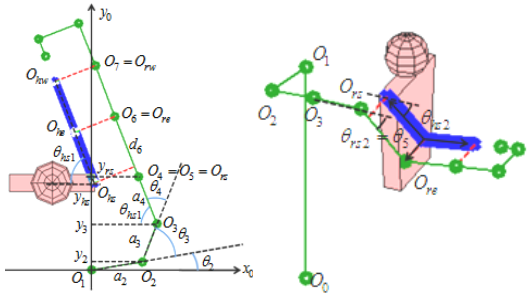

Fig. 7. Figure showing relationship between the rehab-robot and the human arm.

IV. Design of Control System

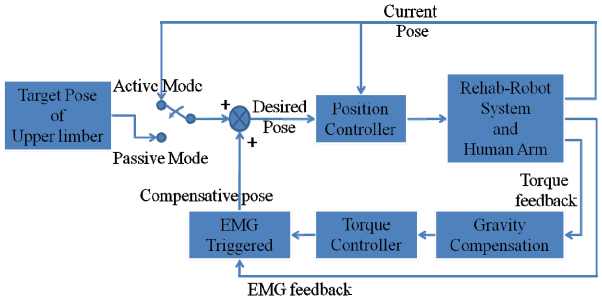

Fig. 8. Control system diagram

Figure 8 shows the control system for two rehabilitation mode, which consists of local PID feedback controller, impedance controller, EMG-trigger, and a switch. The local PID feedback controller is position controller which receives the error between the desired and the current pose of rehab-robot and endeavors to drive the error to zero. The impedance controller is the torque controller, which tries to minimize the torque/force interaction between the rehab-robot and the human arm as much as possible, thus

driving the rehab-robot to follow the human volition to move. The EMG- trigger is used to check whether the human muscles are shrunk. Finally, the switch can choose the between the active mode and passive mode.

A. Local PID Feedback Control

Because the precision level of position control of the rehab-robot during rehabilitation therapy is not required to be as high as that of industrial manipulator, here we choose local PID feedback controller to control the robot arm. The controller is shown mathematically in the following :

Subject to this controller, not only the computational burden can be dramatically reduced, but also the tracking error is kept bounded if appropriate feedback gains are chosen. The detailed discussion and proof can be shown in [10].

B. Impedance Controller

The use of impedance control is to imitate mechanical impedance between the pose and torque of human upper limb. The general form is shown as follows :

$$\tau = M_m(\ddot{\theta}_d - \ddot{\theta}) + B_m(\dot{\theta}_d - \dot{\theta}) + K_m(\theta_d - \theta) \tag{19}$$

where τ is defined as torques due to movements of upper limb, θ is the current pose of human upper limb, θ_d is the desired pose of human upper limb and M_m, B_m, K_m are inertia, damping, and stiffness, respectively.

We assume the imitated inertia and damping of mechanical impedance are zero if the speed of rehabilitation motion is slow. The function (19) can then be simplified into the following :

$$\theta_d = \theta + \frac{\tau}{K_m} = \theta + \Delta\theta_\tau \tag{20}$$

The physical meaning of eq. (20) is that the desired pose is the current pose plus the compensated pose $\Delta\theta_\tau$, which on the other hand means that the desired pose shall follow the direction of torque.

C. EMG-Triggered

The EMG equipment is used to detect the weak EMG signals produced by the stroke patients. But the force sensor is a transducer that converts an input mechanical force into electrical output signals. Therefore, by a comparison between the EMG signals and the electrical signals of the mechanical force sensors produced by the stroke patients, this system can detect the right muscle contractions and then the rehab-robot provides stroke patients with right external force that assists them to complete the designated tasks. The details are described as follows:

1) EMG Pre-processing: We record EMG singles $m_{ch}(t)$ with a band pass from 20 Hz to 450 Hz, and the myoelectric activity $E_{ch}(t)$ is defined as follows:

$$E_{ch}(t) = \sqrt{\frac{1}{T}\int_{t-T}^{t} {m_{ch}}^2(t)dt} \tag{21}$$

where $ch = 1, 2, \cdots, 8$ indicates the specific muscle.

2) Triggered signal definition: The threshold T_{ch} is decided by myoelectric activity of the relaxed muscle, and the triggered signal is defined as follows:

$$TC_{mov}(t) = \begin{cases} 1, & if \prod_{ch \in mov} E_{ch}(t) > T_{ch} \\ 0, & otherwise \end{cases} \tag{22}$$

where mov is the set of channels which indicate the specific muscles, and these specific muscles are responsible for specific movement of upper limb.

Then, the control strategy (21) will be modified to reflect the incorporation of EMG-trigger as follows :

$$\theta_d(t) = \theta(t) + TC(t) \cdot \frac{\tau}{K} \tag{23}$$

where $TC(t)$ is defined as the triggered signals which are responsible for specific movements of upper limb

V. Experimental and Result

A. Experimental Setup

This experiment of circle drawing is executed by one subject from this rehab-robot design group, and LabVIEW 8.6 is used for programming.

Circle drawing in the frontal plane is a training program. During practice of circle drawing, the rehabilitation modes can be selected including the passive mode and the active mode.

Before executing the task of circle drawing, the rehab-robot should be setup first. The shoulder and elbow joints of the rehab-robot are set in the initial position and the lengths of rehab-robot upper arm and forearm are appropriately adjusted. Then, the subject sits with his upper arm and forearm attached to the support base immobilized by straps, and his hand grasps the handle. Surface EMG electrodes are attached to the skin surface of the subject, including deltoid muscle (anterior, middle, and posterior part), the biceps brachii muscle, and the triceps brachii muscle. These muscles are responsible for shoulder flexion/extension, abduction, and elbow flexion/ extension. The EMG noise level is measured as the threshold value during the resting state.

After setting up the rehab-robot, the task of circle drawing with visual feedback from the computer screen is executed in each rehabilitation mode. Besides, up to shoulder level, the diameter of the target circle is set as 24 cm in clockwise

rotation. The speed of circle drawing can be self-determined, and the subject follows the circle track shown on the computer.

B. Results

Under the three different modes, Figs. 9 show the trajectory of wrist in xz-plane and yz-plane. And then, the angle of human's upper-limb Figs. 10 also in two different modes.

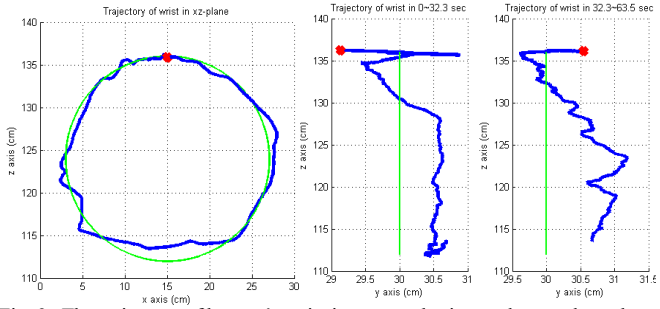

Fig. 9. The trajectory of human's wrist in two modes in xz-plane and yz-plane. The smooth path is the trajectory of passive mode, the irregular one is of active mode.

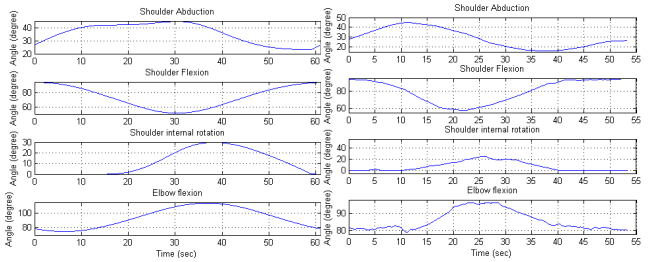

Fig. 10. The angle of human's upper-limb versus time in passive mode (left figure) and active mode (right figure).

VI. Discussion

From Figs. 9, we can clearly see that the circular trajectory of active mode is not smoother than that of passive mode. This is because to let the subject position his/her wrist along a pre-defined path through display from a low resolution screen is indeed not easy in the experiments. In particular, the depth value (y-axis) of the wrist seems to drift a lot in the active mode. So the circle drawing in the active mode provides an advanced training for patients with minor paresis, and passive mode are to be used in severe paresis.

From Figs. 10, one can see that the tendencies of shoulder flexion and elbow flexion are similar, but the tendencies of shoulder abduction and internal rotation are different in three modes. This should be attributed to the different strategy for resolving the redundancy. The strategy in passive mode is to adopt the minimum movement of elbow, whereas in active mode is to give authority to the subject. Based on these results, we can analyze the variation of motor control strategies in the long-term training.

VII. Conclusions and Future Work

We designed an exoskeleton-type rehabilitation robot (rehab-robot) with redundancy and it does not need special component like the circular guide which is used to drive the human shoulder rotation. Also presented is the redundancy design combined with selective inverse kinematic (IK) solutions, and the torque feedback with EMG-trigger. An application to circle drawing task is implemented our future work is to design the controller which can guide the patient to trace the circular path and train the patient's motor control strategy for moderate paresis.

Acknowledgment

We would like to thank the Medical team and all rehabilitation therapists of National Taiwan University Hospital for their assistance and valuable efforts on the latest prototype development of upper limb rehab-robot.

References

[1] H.I. Krebs, N. Hogan, B.T. Volpe, M.L. Aisen, L. Edelstein, and C. Diels, "Overview of clinical trials with MIT-MANUS: a robot-aided neuro-rehabilitation facility," *Technol . Health Care*, vol. 7, 1999, pp. 419-23.

[2] M. Bergamasco, B. Allotta, L. Bosio, L. Ferretti, G. Parrini, G. Prisco, F. Salsedo, and G. Sartini, "An arm exoskeleton system for teleoperation and virtual environments applications," in *Proc. IEEE Int. Conf. Robot. Autom.*, vol. 2, 1994, pp. 1449–1454.

[3] M. Mihelj, T. Nef, and R. Riener, "ARMin II - 7 DoF rehabilitation robot: mechanics and kinematics," in *Proc. IEEE Int. Conf. on Robotics and Automat.*, Roma, Italy, 2007, pp. 4120-4125.

[4] Y. Yong, W. Lan, T. Jie, and Z. Lixun, "Arm Rehabilitation Robot Impedance Control and Experimentation," in *Proc. IEEE Int. Conf. on Robotics and Biomimetics*, 2006, pp. 914-918.

[5] D. Formica, L. Zollo, and E. Guglielmelli, "Torque-dependent compliance control in the joint space for robot-mediated motor therapy," *Journal of Dynamic Systems, Measurement and Control*, vol. 128, (1), 2006, pp. 152-158.

[6] H.I. Krebs, J.J. Palazzolo, L. Dipietro, B.T. Volpe, and N. Hogan, "Rehabilitation robotics: Performance-based progressive robot-assisted therapy," *Autonomous Robots*, vol. 15, 2003, pp. 7-20.

[7] L. Dipietro, M. Ferraro, J.J. Palazzolo, H.I. Krebs, B.T. Volpe, and N. Hogan, "Customized interactive robotic treatment for stroke: EMG-triggered therapy," *IEEE Trans. on Neural Systems and Rehabilitation Engineering*, vol. 13, 2005, pp. 325-334.

[8] T. Miyoshi, Y. Takahashi, H. Lee, T. Suzuki, and T. Komeda, "Upper limb neurorehabilitation in patients with stroke using haptic device system: Reciprocal bi-articular muscle activities reflect as a result of improved circle-drawing smoothness," *Disabil Rehabil Assist Technol*, vol. 5, 2010, pp. 370-375.

[9] S.M. Lewis, T.A. Jerde, C. Tzagarakis, M.A. Georgopoulos, N. Tsekos, B. Amirikian, S.G. Kim, K. Ugurbil, and A.P. Georgopoulos, "Cerebellar activation during copying geometrical shapes," *J. Neurophysiol*, vol. 90, 2003, pp. 3874-3887.

[10] L.-C. Fu, "Stability analysis of independent joint PID feedback control for trajectory tracking of Robot motion," *Chinese Institute of Engineers*, vol. 14, 1991, pp. 9-20.